Carbohydrate Polymers 79 (2010) 206–213

Contents lists available at ScienceDirect

Carbohydrate Polymers

journal homepage: www.elsevier.com/locate/carbpol

Medium optimization and structural characterization of exopolysaccharides from endophytic bacterium *Paenibacillus polymyxa* EJS-3

Jun Liu, Jianguang Luo, Hong Ye, Yi Sun, Zhaoxin Lu, Xiaoxiong Zeng *

College of Food Science and Technology, Nanjing Agricultural University, Nanjing, 210095 Jiangsu, China

ARTICLE INFO

Article history:
Received 23 June 2009
Received in revised form 26 July 2009
Accepted 29 July 2009
Available online 3 August 2009

Keywords:
Paenibacillus polymyxa
Endophytic bacterium
Exopolysacchrides
Response surface methodology
Structural characterization

ABSTRACT

In this study, response surface methodology was employed to optimize the medium compositions for the production of exopolysaccharides (EPS) from endophytic bacterium *Paenibacillus polymyxa* EJS-3. Firstly, fractional factorial design was applied to evaluate the effects of different components in the medium. It was found that sucrose, yeast extract and $CaCl_2$ influenced significantly the production of EPS. Then, steepest ascent method and central composite design were used to optimize the concentrations of the three variables. As results, the optimal medium compositions were determined as following (g/L): sucrose 188.2, yeast extract 25.8, K_2HPO_4 5 and $CaCl_2$ 0.34, with a corresponding yield of 35.26 g/L. In addition, both polysaccharide fractions (EPS-1 and EPS-2) from crude EPS were mainly composed of (2 → 6)-linked β-D-fructofuranosyl residues backbone with (2 → 1)-linked branches based on their structural characterization by FT-IR spectroscopy, methylation analysis and ^{13}C NMR spectroscopy.

1. Introduction

Endophytic microorganisms that asymptomatically lived in the intracellular spaces of higher plants have recently been intensified due to their potentialities in the production of bioactive and structurally novel metabolites (Tadych & White, 2009). A number of bioactive products such as antibiotics, antiviral, anticancer and antidiabetic agents have been isolated from endophytes (Guo, Wang, Sun, & Tang, 2008). In addition, exopolysaccharides (EPS) produced by endophytes are also important metabolites, which play key roles in plant–endophyte interactions (Mattos, Jones, Heise, Previato, & Mendonça-Previato, 2001; Serrato et al., 2006). They provide the endophytes additional protection against desiccation and serve as molecular signals during plant invasion (Serrato et al., 2008). Despite the growing understanding on the role of EPS in the establishment of interactions, only few reports on the culture conditions, structural characterizations and biological activities of EPS from endophytes are available to date (Mattos et al., 2001; Serrato et al., 2006, 2008). In order to better exploit and utilize this kind of new resource, it is essential to further investigate into EPS produced by endophytes.

Paenibacillus polymyxa (previously *Bacillus polymyxa*) EJS-3 is an endophytic bacterium isolated from the root tissue of *Stemona japonica* (Blume) Miquel, a traditional Chinese medicine (Lu et al., 2007). Recently, we reported the culture conditions, monosaccharide compositions and antioxidant activity *in vitro* of EPS from *P. polymyxa* EJS-3 (Liu et al., 2009). We found that sucrose and yeast extract were the suitable carbon and nitrogen sources for EPS production, respectively. In addition, both crude and purified EPS exhibited strong scavenging activities on superoxide and hydroxyl radicals *in vitro*. In our previous report, effects of various culture conditions (initial pH, temperature, carbon and nitrogen sources) on EPS production were investigated by single factor method (Liu et al., 2009). Notably, the single factor method is tedious and overlooks the interaction between different variables involved (Francis et al., 2003). Alternatively, response surface methodology (RSM) is a well-known method applied in the optimization of medium compositions and other critical variables responsible for the production of biomolecules (Banik, Santhiagu, & Upadhyay, 2007). It is a powerful technique for testing multiple variables because fewer experimental trails are needed compared to single factor method. In addition, the interaction between different variables can be identified by this technique (Shih, Yu, Hsieh, & Wu, 2009). Till now, RSM has been successfully applied in the optimization of medium compositions for EPS production (Banik et al., 2007; Majumder, Singh, & Goyal, 2009; Shih et al., 2009).

In order to better exploit EPS from *P. polymyxa* EJS-3, we optimized the medium compositions for EPS production by RSM and further characterized its structure in this study. Firstly, fractional factorial design (FFD) was applied to screen the most significant variables affecting EPS production based on the previous single factor experiment. Then, the steepest ascent method and central composite design (CCD) were used to search the optimum medium compositions for maximum EPS production. Finally, Fourier-transform infrared (FT-IR) spectroscopy, methylation

* Corresponding author. Fax: +86 25 84396791.
E-mail address: zengxx@njau.edu.cn (X. Zeng).

0144-8617/$ - see front matter © 2009 Elsevier Ltd. All rights reserved.
doi:10.1016/j.carbpol.2009.07.055

analysis and ^{13}C nuclear magnetic resonance (NMR) spectroscopy were used for the structural characterization of EPS. The complex formation of EPS with Congo Red was also evaluated.

2. Materials and methods

2.1. Microorganism and medium

Paenibacillus polymyxa EJS-3 used in this study was provided by the Laboratory of Enzyme Engineering, Nanjing Agricultural University. The strain was cultured on potato dextrose agar (PDA) slant at 28 °C for 1 day, and then maintained at 4 °C. The seed culture medium contained (g/L): sucrose 30, yeast extract 5, meat peptone 5, K_2HPO_4 3, KH_2PO_4 1, $MgSO_4$ 0.5, and initial pH at 7.0. The fermentation medium contained (g/L): sucrose 150, yeast extract 15, K_2HPO_4 5 and $CaCl_2$ 0.55, and initial pH at 8.0.

2.2. Culture conditions

Inoculum was prepared by transferring one loop full of culture from PDA slant to an Erlenmeyer flask (250 ml) containing 50 ml seed medium. The seed cultures were grown at 28 °C on a rotary shaker incubator at 180 rpm for 18 h. After incubation, 3 ml of the seed culture was transferred into an Erlenmeyer flask (250 ml) containing 50 ml of fermentation medium. The fermentation cultures were then incubated at 24 °C with shaking at 150 rpm for 60 h.

2.3. Determination of EPS production

Samples collected from the fermentation broth was properly diluted and centrifuged at 10,000 rpm for 15 min. The resulting supernatant was filtered through a 0.45 μm membrane filter, mixed with four volumes of anhydrous ethanol, stirred vigorously and kept overnight at 4 °C. The precipitate from the ethanol dispersion was collected by centrifugation at 10,000 rpm for 15 min, redissolved in distilled water and followed by deproteinization with 1/5 volume of Sevag reagent ($CHCl_3$–BuOH, v/v = 5/1) for seven times (Staub, 1965). The deproteinized solution was then dialyzed against distilled water, concentrated, lyophilized to afford the crude EPS. The weight of crude EPS was determined.

2.4. Experimental designs

2.4.1. Fractional factorial design

In our previous report, four variables (sucrose, yeast extract, K_2HPO_4 and $CaCl_2$) having effects on EPS production were identified by single factor experiment (Liu et al., 2009). Here, the variables having the most significant effects on EPS production were determined using a two-level FFD. According to the FFD, each variable was examined at two levels: −1 for low level and +1 for high level, and a center point (0) was run to evaluate the linear and curvature effects of variables. Table 1 represents the design matrix of the variables under investigation as well as levels of each variable. FFD was based on the following first-order polynomial model:

$$Y = \beta_0 + \sum \beta_i x_i \quad (1)$$

where Y was the predicted response (EPS production), β_0 was the model intercept, β_i was the linear coefficient and x_i was the level of independent variable. In this study, four variables were screened by eight experimental runs in addition with two runs at the center point. From the regression analysis, the variables significant at 90% of confidence level ($P < 0.10$) were considered to have significant effects on EPS production.

2.4.2. Path of steepest ascent experiment

The variables screened by FFD were further optimized by the method of steepest ascent. The direction of steepest ascent was parallel to the normal of the contour line of model (1) and passed through the center point of FFD. Experiments were performed along the steepest ascent path until the response did not increase any more. And this point would be near the optimal point and could be used as the center point of CCD (Tang, He, Chen, Zhang, & Ali, 2004). Table 2 shows the experimental design and corresponding response of the steepest ascent path.

2.4.3. Central composite design

Subsequently, CCD was employed to optimize the three most significant variables (sucrose, yeast extract and $CaCl_2$) to further enhance EPS production. The three independent variables were studied at five different levels (−1.68, −1, 0, +1 and +1.68) and a set of 20 experiments were carried out as shown in Table 3. The relationships and interrelationships of the variables were based on the following second-order polynomial model:

$$Y = \beta_0 + \sum \beta_i x_i + \sum \beta_{ii} x_i^2 + \sum \beta_{ij} x_i x_j \quad (2)$$

where Y was the predicted response (EPS production), β_0 was the model intercept, x_i and x_j were the level of independent variable, β_i, β_{ii}, and β_{ij} were the linear, quadratic and interaction coefficients, respectively.

2.4.4. Data analysis

Design Expert software of version 7.0 (Stat-Ease Inc., Minneapolis, USA) was used for the experimental designs and regression analysis of the experimental data. Statistical analysis of the model was performed to evaluate the analysis of variance (ANOVA). The quality of the polynomial model equation was judged by determination coefficient R^2, and its statistical significance was determined

Table 1
Coded levels and real values (in the parentheses) for the experimental design and results of FFD.

Run	Coded levels (real values)				EPS (g/L)	
	Sucrose (g/L)	Yeast extract (g/L)	K_2HPO_4 (g/L)	$CaCl_2$ (g/L)	Observed	Predicted
1	−1 (100)	−1 (10)	+1 (8)	+1 (1.0)	10.46	13.44
2	+1 (200)	−1 (10)	+1 (8)	−1 (0.1)	30.92	29.92
3	−1 (100)	−1 (10)	−1 (2)	−1 (0.1)	19.87	18.52
4	+1 (200)	+1 (20)	−1 (2)	−1 (0.1)	34.00	36.98
5	+1 (200)	−1 (10)	−1 (2)	+1 (1.0)	24.49	23.84
6	−1 (100)	+1 (20)	+1 (8)	−1 (0.1)	27.23	26.58
7	−1 (100)	+1 (20)	−1 (2)	+1 (1.0)	21.48	20.50
8	+1 (200)	+1 (20)	+1 (8)	+1 (1.0)	33.24	31.90
9	0 (150)	0 (15)	0 (5)	0 (0.55)	24.40	25.21
10	0 (150)	0 (15)	0 (5)	0 (0.55)	24.96	25.21

Table 2
Experimental design and results of the steepest ascent path.

Run	Sucrose (g/L)	Yeast extract (g/L)	$CaCl_2$ (g/L)	EPS (g/L)
Origin	150	15	0.55	24.77
1	160	17.5	0.50	27.98
2	170	20	0.45	30.63
3	180	22.5	0.40	32.89
4	190	25	0.35	35.45
5	200	27.5	0.30	32.55
6	210	30	0.25	29.38
7	220	32.5	0.20	25.07

by *F*-test. The significance of the regression coefficients was tested by *t*-test.

2.5. Structural characterization of EPS

In our previous report, the crude EPS from *P. polymyxa* EJS-3 was purified by chromatography of DEAE-52 and Sephadex G-100, affording EPS-1 and EPS-2 with molecular weights of 1.22×10^6 and 8.69×10^5 Da, respectively. In addition, EPS-1 and EPS-2 were composed of mannose, fructose and glucose in a molar ratio of 2.59:29.83:1 and 4.23:36.59:1, respectively, by GC–MS analysis of monosaccharide composition (Liu et al., 2009). In this study, the structures of EPS-1 and EPS-2 were further characterized by FT-IR spectroscopy, methylation analysis, ^{13}C NMR spectroscopy and helix–coil transition assay.

2.5.1. FT-IR spectrometric analysis

FT-IR spectra of EPS-1 and EPS-2 were recorded on a Tensor-27 FT-IR spectrometer (Bruker Optics, Wissembourg, France). The dried sample was grinded with potassium bromide (KBr) powder and pressed into pellet for spectrometric measurement in the frequency range of 4000–400 cm^{-1}.

2.5.2. Methylation and GC–MS analysis

Methylation of EPS-1 and EPS-2 were performed according to the method described by Ciucanu and Kerek (1984). Complete methylation was confirmed by the lack of hydroxyl peak in FT-IR spectrum. The permethylated polysaccharide was hydrolyzed with trifluoroacetic acid at 60 °C for 30 min (Wack & Blaschek, 2006). Then the methylated sugars were reduced with $NaBH_4$ and acetylated with acetic anhydride. The resulting partially methylated alditol acetate derivatives were analyzed by GC–MS.

GC–MS analysis was performed on a Varian CP-3800 gas chromatograph coupled with a Saturn 2000 ion trap mass spectrometer (Walnut Creek, CA, USA). A DB-5 fused silica capillary column (30 m × 0.25 mm × 0.25 mm, J&W Scientific, Folsom, CA, USA) was used with He as carrier gas. The oven temperature was initially set at 100 °C, programmed at 6 °C/min to 250 °C and held at 250 °C for 5 min.

2.5.3. ^{13}C NMR spectral analysis

^{13}C NMR spectra of EPS-1 and EPS-2 were recorded on a Bruker AV-500 NMR spectrometer with an operating frequency of 125 MHz at 30 °C for 8 h. Samples were prepared by dissolving 10 mg of EPS-1 or EPS-2 in 0.5 ml D_2O (99.9%). The carbon signals were assigned by comparison with the chemical shifts in literature reported (Chen & Tian, 2003; Cunha, Vieira, Arriaga, de Paula, & Feitosa, 2009; Han & Clarke, 1990; Kardošová et al., 2003; Tajima et al., 1998; Wack & Blaschek, 2006).

2.5.4. Helix–coil transition assay

Helix–coil transition assay using Congo Red dye was performed according to the method described by Ogawa, Wanatabe, Tsurugi, and Ono (1972). The solutions of EPS-1 or EPS-2 (1 mg/ml) in 0.05–0.40 M NaOH containing 91 μmol of Congo Red were prepared. After reaction for 3 h, the visible absorption spectra were recorded from 400 to 700 nm at 25 °C with a Shimadzu UV-2450 spectrophotometer (Shimadzu, Kyoto, Japan).

3. Results and discussion

3.1. Evaluation of variables affecting EPS production by FFD

In our previous study, we used single factor method to evaluate various factors affecting EPS production by *P. polymyxa* EJS-3. Experimental data showed that the variables affecting EPS production were the levels of sucrose, yeast extract, K_2HPO_4 and $CaCl_2$ (Liu et al., 2009). In this study, FFD was used first to screen the relatively significant variables for EPS production. As shown in Table 1, the EPS yields varied markedly from 10.46 to 34.00 g/L under different levels of medium components. This variation reflected the importance of medium optimization to attain maxi-

Table 3
Coded levels and real values (in the parentheses) for the experimental design and results of CCD.

Run	Coded levels (real values)			EPS (g/L)	
	Sucrose (g/L)	Yeast extract (g/L)	$CaCl_2$ (g/L)	Observed	Predicted
1	0 (190)	0 (25)	0 (0.35)	34.84	35.62
2	−1 (180)	1 (27.5)	1 (0.40)	33.45	33.80
3	0 (190)	1.68 (29.2)	0 (0.35)	34.39	34.54
4	0 (190)	0 (25)	0 (0.35)	35.45	35.62
5	0 (190)	0 (25)	0 (0.35)	35.89	35.62
6	−1 (180)	1 (27.5)	−1 (0.30)	34.72	34.32
7	1.68 (206.82)	0 (25)	0 (0.35)	29.85	29.71
8	1 (200)	1 (27.5)	1 (0.40)	32.22	32.51
9	1 (200)	−1 (22.5)	1 (0.40)	31.86	32.51
10	1 (200)	1 (27.5)	−1 (0.30)	31.75	32.23
11	−1.68 (173.18)	0 (25)	0 (0.35)	30.69	31.38
12	0 (190)	0 (25)	0 (0.35)	35.79	35.62
13	0 (190)	0 (25)	1.68 (0.43)	34.46	34.55
14	1 (200)	−1 (22.5)	−1 (0.30)	32.50	32.40
15	−1 (180)	−1 (22.5)	1 (0.40)	32.63	32.40
16	−1 (180)	−1 (22.5)	−1 (0.30)	33.14	33.10
17	0 (190)	0 (25)	−1.68 (0.27)	34.23	34.88
18	0 (190)	−1.68 (20.8)	0 (0.35)	33.11	33.52
19	0 (190)	0 (25)	0 (0.35)	35.54	35.62
20	0 (190)	0 (25)	0 (0.35)	35.12	35.62

Table 4
ANOVA for response surface quadratic model.

Source	Sum of squares	Degrees of freedom	Mean square	*F*-Value	*P*-Value
Model	55.23	9	6.14	25.93	<0.0001[a]
Residual	2.37	10	0.24		
Lack of fit	1.57	5	0.31	1.97	0.2378
Pure error	0.80	5	0.16		
Total	57.59	19			
A	3.61	1	3.61	15.26	0.0029[a]
B	1.27	1	1.27	5.36	0.0431[a]
C	0.18	1	0.18	0.76	0.4049
AB	0.97	1	0.97	4.11	0.0701[a]
AC	0.32	1	0.32	1.37	0.2691
BC	0.015	1	0.015	0.065	0.8044
A^2	46.40	1	46.40	196.08	<0.0001[a]
B^2	4.58	1	4.58	19.37	0.0013[a]
C^2	1.80	1	1.80	7.61	0.0201[a]

[a] Significance at 0.10 level.

mum EPS production. From the regression analysis of the variables, sucrose, yeast extract, and K_2HPO_4 were found to display positive effects on EPS production, whereas $CaCl_2$ display a negative effect on EPS production. The variables with confidence levels greater than 90% ($P < 0.10$) were considered as significant. Thus, sucrose ($P = 0.0123$), yeast extract ($P = 0.0329$) and $CaCl_2$ ($P = 0.0690$) were the most significant variables affecting EPS production. The polynomial model describing the correlation between the four variables and EPS production could be presented as:

$$Y = 25.21 + 5.45X_1 + 3.78X_2 + 0.25X_3 - 2.79X_4 \quad (3)$$

where Y was the predicted response (EPS production), X_1, X_2, X_3 and X_4 were coded values of sucrose, yeast extract, K_2HPO_4 and $CaCl_2$, respectively.

The statistical significance of the model was evaluated by *F*-test, and *P*-value of 0.0313 revealed that the model was significant. The determination coefficient R^2 of the model was 0.9437, indicating that 94.37% of the variability in the response could be explained by the model. However, the results of *t*-test for variance between average of observation of two-level experiment and center point showed that the difference was not significant. This indicated that the optimum center point was outside the domain of our experiment. Thus, the steepest ascent experiment should be performed to reach the optimum domain of the maximum response.

3.2. The steepest ascent experiment and analysis

The path of steepest ascent started from the center point of FFD and moved along the path in which the concentration of sucrose and yeast extract increased, while $CaCl_2$ decreased. K_2HPO_4 was fixed at the center point (5 g/L). Experimental design of the steepest ascent and corresponding results are shown in Table 2. It was evident that the highest EPS production was obtained in Run 4, indicating that it was near the region of the maximum EPS production. Thus, the combination of Run 4 was selected as the center point of CCD.

3.3. Optimization of EPS production by CCD and response surface analysis

Based on FFD and steepest ascent experiments, three variables including sucrose, yeast extract, and $CaCl_2$ were further investigated for their optimum concentrations by CCD. The design matrix and the corresponding results of CCD are shown in Table 3. By employing multiple regression analysis on the experimental data, the predicted response Y for EPS production could be obtained by the following second-order polynomial equation:

$$Y = 35.43 - 0.51A + 0.30B - 0.11C - 0.35AB + 0.20AC + 0.044BC - 1.79A^2 - 0.56B^2 - 0.35C^2 \quad (4)$$

where Y was the predicted response, A, B and C were coded values of sucrose, yeast extract and $CaCl_2$, respectively.

The statistical significance of the model was checked by *F*-test, and ANOVA for response surface quadratic model are summarized in Table 4. A *P*-value less than 0.0001 demonstrated the model was highly significant. The determination coefficient R^2 of the model was 0.9589, indicating that 95.89% of the variability in the response could be explained by the model. Meanwhile, relatively lower value of coefficient of variation (CV, 1.45%) indicated good precision and reliability of the experiments being carried out. In addition, the *P*-value for lack of fit ($P = 0.2378$) implied the lack of fit was not significant relative to the pure error, indicating that the model equation was adequate for predicting EPS production under any combination of values of the variables. Furthermore, the high degree of similarity between the predicted and experimental values also reflected the accuracy and applicability of RSM for medium optimization to attain maximum EPS production.

The significance of the regression coefficients was tested by *t*-test, and the corresponding *P*-values for the model terms are also presented in Table 4. When *P*-value is less than 0.10, the model terms are significant. In this case, A, B, AB, A^2, B^2, C^2 were significant model terms.

The response surface plots and their contour plots are the graphical representations of the regression equation. They provide a visual interpretation of the interaction between two variables and facilitate the location of optimum experimental conditions. The response surface with circular contour plot indicates the interaction between the corresponding variables is negligible, whereas elliptical or saddle nature of the contour plots indicates the interactions between the corresponding variables is significant. In this case, the interaction between sucrose and yeast extract was significant (Fig. 1d). However, the interactions between sucrose and $CaCl_2$, yeast extract and $CaCl_2$ were negligible (Fig. 1e and f). The optimum levels of the variables were obtained by analyzing the response surface contour plots using Design Expert software. The model predicted the maximum EPS production (35.54 g/L) appeared at sucrose 188.2 g/L, yeast extract 25.8 g/L and $CaCl_2$ 0.34 g/L. In order to validate the adequacy of the model equation, three additional experiments in shake flasks under the optimum medium compositions were performed. The mean value of EPS production was 35.26 g/L, which was in good agreement with the predicted value. The yield of EPS was about 1.55-fold compared with that (22.82 g/L) using the original medium (Liu et al., 2009). Therefore, the final medium composition optimized was determined (g/L): sucrose 188.2, yeast extract 25.8, K_2HPO_4 5 and $CaCl_2$ 0.34.

Till now, there have been many reports on the medium compositions for EPS production from *P. polymyxa* (Han & Clarke, 1990; Lee et al., 1997). However, it should be noted that these EPS-producing strains were isolated from soil. In addition, medium compositions for EPS production were optimized by single factor method which ignored the interactions between different variables and involved a relatively large number of experiments. In this study, RSM was used for the first time to optimize the medium compositions for EPS production from *P. polymyxa*. The results indicated that *P. polymyxa* EJS-3 could be a promising EPS producer with potential industrial applications.

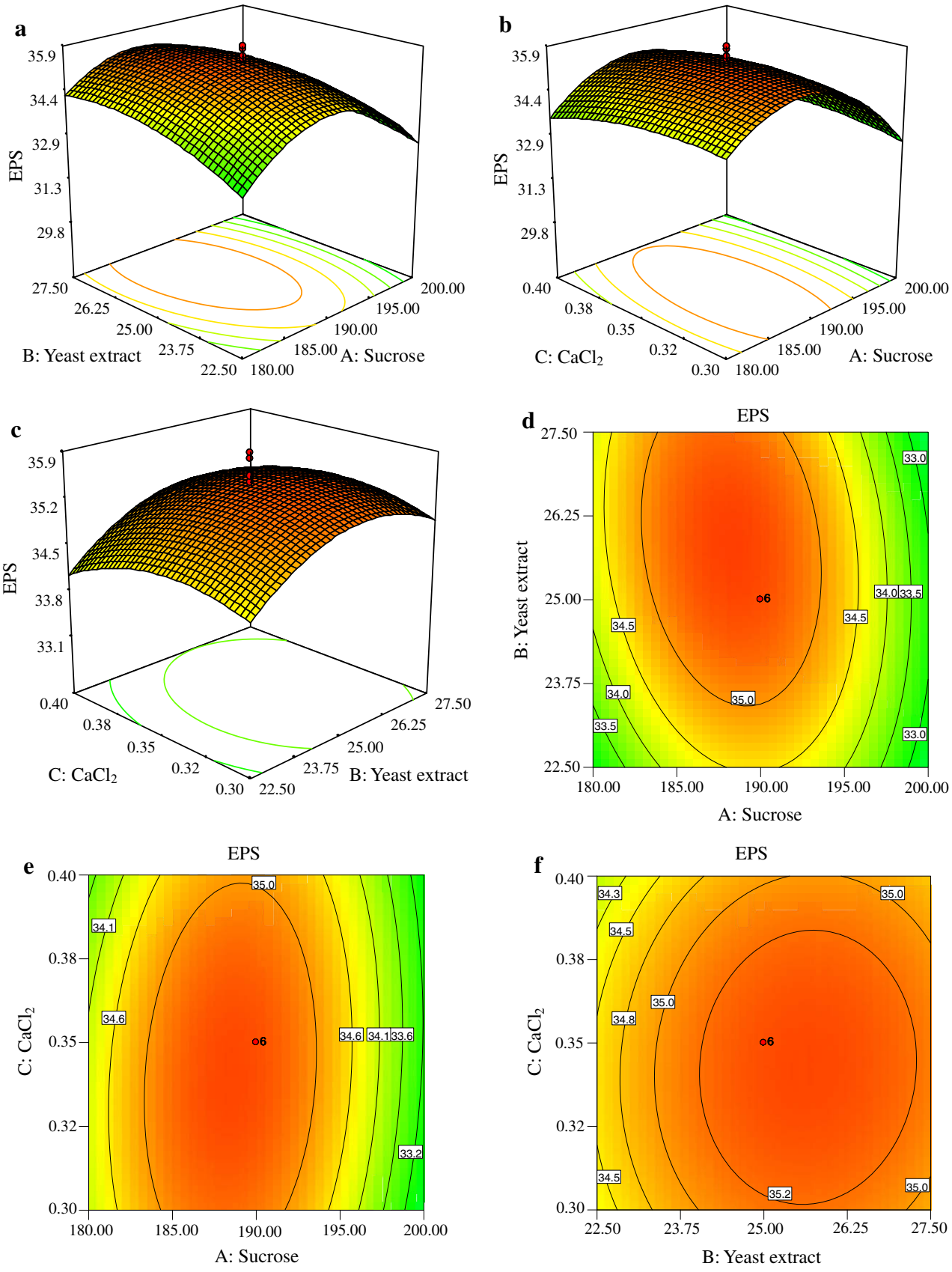

Fig. 1. Response surface plots (a, b and c) and contour plots (d, e and f) showing the effects of sucrose, yeast extract and $CaCl_2$ on EPS production.

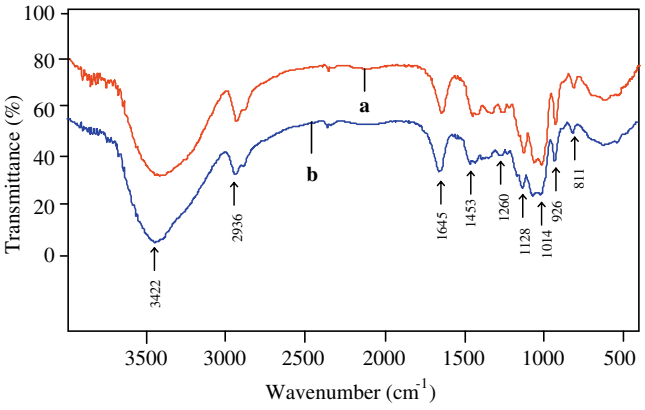

Fig. 2. FT-IR spectra of EPS-1 (a) and EPS-2 (b) from *P. polymyxa* EJS-3.

3.4. Structural characterization of EPS

In our previous report, it has been demonstrated that EPS from *P. polymyxa* EJS-3 had strong scavenging activities on superoxide and hydroxyl radicals (Liu et al., 2009). As the biological activity of EPS is closely related to its chemical structure, it is necessary to characterize the structure of EPS more in detail. Therefore, the structures of EPS-1 and EPS-2 were further characterized by FT-IR spectroscopy, methylation analysis, ^{13}C NMR spectroscopy and helix–coil transition assay.

In order to investigate the functional groups in EPS-1 and EPS-2, their FT-IR spectra were measured in KBr pellets. As shown in Fig. 2, the strong band at 3422 cm^{-1} was assigned to the hydroxyl stretching vibration of the polysaccharide. The band at 2936 cm^{-1} was due to C–H stretching vibration and the band at 1645 cm^{-1} was due to the bound water. The bands in the region of 1500 and 1200 cm^{-1} were assigned to C–H deformation vibration (Hineno, 1977). The bands between 1128 and 1014 cm^{-1} corresponded to C–O–C and C–O–H stretching vibration (Wu, Wu, Zhou, & Pan, 2009). A characteristic absorption at 926 cm^{-1} was resulted from the stretching vibration of pyran ring (Schwanninger, Rodrigues, Pereira, & Hinterstoisser, 2004). The obvious absorption at 811 cm^{-1} revealed the existence of mannose residue (Lim et al., 2005). And two peaks in the region of 3000 and 2800 cm^{-1} were observed, indicating the existence of fructose residue. In addition, it should be noted that the FT-IR spectra of EPS-1 and EPS-2 were similar, indicating they had similar functional groups.

To determine the linkage of monosaccharides in EPS-1 and EPS-2, they were methylated, hydrolyzed and converted into their corresponding alditol acetates for GC–MS analysis. As summarized in Table 5, EPS-1 and EPS-2 were consisted of similar methylated fragments with different molar ratios. The major derivative for both EPS-1 and EPS-2 was 1,3,4-trimethylated fructose, indicating that EPS-1 and EPS-2 were composed of (2 → 6)-linked β-D-fructofuranosyl (Fru*f*) backbone. In addition, a 3,4-dimethylated derivative of fructose showed the presence of branched residues. The terminal non-reducing fructose, glucose and mannose residues were also observed. These results indicated that EPS-1 and EPS-2 were both composed of β-(2 → 6)-linked backbone of fructose residues, which substituted at C-1 by fructose and mannose residues.

^{13}C NMR spectroscopy was then used to verify the linkages deduced from GC–MS. As shown in Fig. 3a, the ^{13}C NMR spectrum of EPS-1 was almost identical with the peak positions for levan previously identified by Shimamura et al. (1987) and Han and Clarke (1990). The anomeric region of EPS-1 contained a set of resonance between 103.5 and 104.2 ppm, which were deduced to correspond to the C-2 of various β-D-Fru*f* residues. The signals at 104.1 and 104.2 ppm were assigned to (2 → 6)-linked β-D-Fru*f* residues. The occurrence of (2 → 6)-linked β-D-Fru*f* residues was also supported by the signal at 80.3 ppm, which could be attributed to C-5 of such a unit or a branched residue. Another strong evidence for (2 → 6)-linked β-D-Fru*f* residues was the broad signal at 63.4 ppm, which was characteristic of 6-substitution. The signals at 76.3, 75.2 and 59.9 ppm were assigned to C-3, C-4 and C-1 of (2 → 6)-linked β-D-Fruf residues, respectively. In addition, the signals at 103.8–103.9 and 103.5–103.6 ppm were assigned to (2 → 1,6)-linked and terminal β-D-Fruf residues, respectively. These results were in accordance with the linkage deduced by GC–MS. However, the signals for α-D-Glcp and β-D-Manp residues in EPS-1 were not clearly detected due to the small proportion of them. Based on the results of monosaccharide compositions, FT-IR, GC–MS and ^{13}C NMR analysis, it could be deduced that EPS-1 was a levan type polysaccharide, which was consisted of (2 → 6)-linked β-D-Fru*f* residues with (2 → 1)-linked β-D-Fru*f* branches.

In a similar manner, EPS-2 was also identified as a levan type polysaccharide. As shown in Fig. 3b, EPS-2 had almost similar signals as EPS-1. Meanwhile, EPS-2 exhibited additional signals in the anomeric region of 100.6–100.7 ppm, which could be assigned to the C-1 of terminal β-D-Man*p* residues (Cunha et al., 2009). However, the signals for α-D-Glc*p* residues were not detected. It might be due to its small proportion. Therefore, EPS-2 was deduced to be consisted of (2 → 6)-linked β-D-Fru*f* residues with (2 → 1)-linked β-D-Fru*f* and β-D-Man*p* branches.

The complex formation of EPS-1 and EPS-2 with Congo Red was evaluated. According to the method of Ogawa et al. (1972), the helix conformation of polysaccharide can be identified by a red shift in the visible absorption maximum value (λ_{max}) of the Congo Red–polysaccharide complex. However, no considerable shift of λ_{max} for both EPS-1 and EPS-2 was observed (data not shown) in this study. Therefore, it could be concluded that EPS-1 and EPS-2 did not exist helix conformation in their structures.

In general, the structures of EPS produced by *P. polymyxa* are in a great variety, depending on the type of *P. polymyxa* strains and medium compositions. Madden, Dea, and Steer (1986) reported that EPS produced by *P. polymyxa* NCIB 11429 from medium containing sucrose and yeast extract was composed glucose, mannose, galactose, glucuronic acid and pyruvate. While Han and Clarke (1990) found that EPS from *P. polymyxa* NRRL B-18475 in medium containing sucrose, peptone and yeast extract was β-(2 → 6)-

Table 5
GC–MS analysis of partial methylated alditol acetates of EPS-1 and EPS-2.

Linkage	Methylated sugar derivates[a]	Major mass spectral fragments (*m/z*)	Molar ratio (%)	
			EPS-1	EPS-2
Terminal β-D-Man*p*	2,3,4,6-Me$_4$-Man	43, 45, 71, 87, 101, 117, 129, 145, 161, 205	2	7
Terminal α-D-Glc*p*	2,3,4,6-Me$_4$-Glc	43, 45, 71, 87, 101, 117, 129, 145, 161, 205	1	2
Terminal β-D-Fruf	1,3,4,6-Me$_4$-Fru	43, 45, 87, 101, 129, 145, 161, 205	8	6
6-Linked β-D-Fru*f*	1,3,4-Me$_3$-Fru	43, 45, 87, 101, 129, 145, 161, 189, 205	79	72
1,6-Linked β-D-Fru*f*	3,4-Me$_2$-Fru	43, 87, 129, 189	10	13

[a] 2,3,4,6-Me$_4$-Man = 1,5-di-*O*-acetyl-2,3,4,6-tetra-*O*-methyl-manitol.

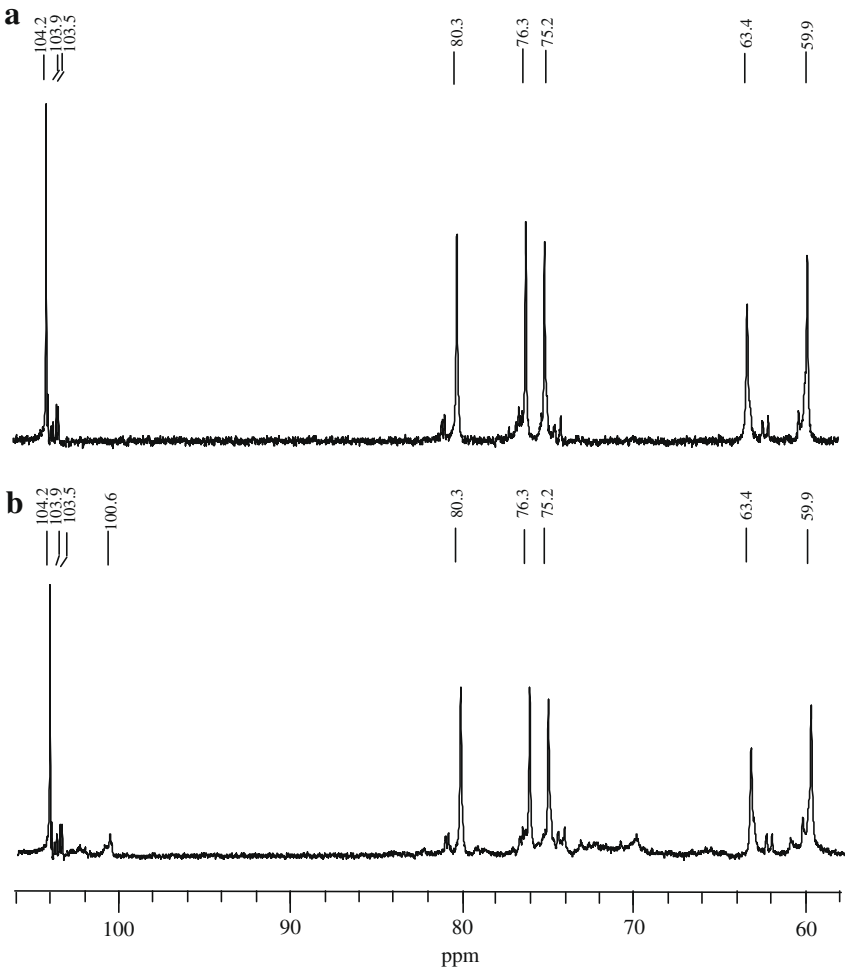

Fig. 3. ^{13}C NMR spectra of EPS-1 (a) and EPS-2 (b) from *P. polymyxa* EJS-3.

linked fructan with a molecular weight of 2×10^6 Da and 12% branching degree. Lee et al. (1997) reported that EPS produced by *P. polymyxa* KCTC 8648P in medium containing sucrose and potassium nitrate was composed of glucose, galactose, mannose, fucose and glucuronic acid. Recently, Recently, Jung et al. (2007) isolated one kind of EPS from *P. polymyxa* JB115 in medium containing sucrose to be β-(1 → 3) and β-(1 → 6)-linked glucan. Here, the EPS from *P. polymyxa* EJS-3 in medium containing sucrose and yeast extract were found to be levan type polysaccharides, somewhat similar to EPS from *P. polymyxa* NRRL B-18475 with different molecular weights and branching degrees.

Except for *P. polymyxa*, many other microorganisms including *Pseudomonas* sp., *Bacillus* sp., *Zymomonas* sp., *Microbacterium* sp., and *Streptococcus* sp. have been reported to produce levans (Yoo, Yoon, Cha, & Lee, 2004). Recently, increasing evidences have shown that levans from different microorganisms possess various biological activities and could have a wide of applications (Arvidson, Rinehart, & Gadala-Maria, 2006). They can be used in medicine as hypo-cholesterol, antitumor, immune modulator, anti-inflammatory and plasma substitute agents (Yoo et al., 2004). Moreover, levans can also be used in food as emulsifiers, stabilizers, thickeners and encapsulating agents (Bekers et al., 2005). In this study, structural characterization of EPS-1 and EPS-2 from *P. polymyxa* EJS-3 showed that they were levan type polysaccharides, indicating that they could have a wide of applications in medicinal and food industries. Furthermore, our previous study demonstrated that EPS had scavenging effects on superoxide and hydroxyl radicals (Liu et al., 2009). To better utilize this kind of resource, further works on physical and other biological activities of EPS from *P. polymyxa* EJS-3 is in progress.

4. Conclusion

In this study, the medium composition for EPS production from endophytic bacterium *P. polymyxa* EJS-3 was optimized by RSM to be sucrose 188.2 g/L, yeast extract 25.8 g/L, K_2HPO_4 5 g/L, and $CaCl_2$ 0.34 g/L. The maximum EPS production was 35.26 g/L, which was 1.55-fold compared with that using original medium. The results indicated that it could be a new source for the production of bioactive polysaccharide. Furthermore, both polysaccharide fractions (EPS-1 and EPS-2) from crude EPS were identified to be levan type polysaccharides based on their structural characterization by FT-IR spectroscopy, methylation analysis and ^{13}C NMR spectroscopy.

Acknowledgements

This work was partly supported by Grants-in-Aid for scientific research from the National Natural Science Foundation of China (Nos. 30570415 and 30870547).

References

Arvidson, S. A., Rinehart, B. T., & Gadala-Maria, F. (2006). Concentration regimes of solutions of levan polysaccharide from *Bacillus* sp. *Carbohydrate Polymers, 65*, 144–149.

Banik, R. M., Santhiagu, A., & Upadhyay, S. N. (2007). Optimization of nutrients for gellan gum production by *Sphingomonas paucimobilis* ATCC-31461 in molasses

based medium using response surface methodology. *Bioresource Technology, 98*, 792–797.
Bekers, M., Upite, D., Kaminska, E., Laukevics, J., Grube, M., Vigants, A., et al. (2005). Stability of levan produced by *Zymomonas mobilis*. *Process Biochemistry, 40*, 1535–1539.
Chen, X. M., & Tian, G. Y. (2003). Structural elucidation and antitumor activity of a fructan from *Cyathula officinalis* Kuan. *Carbohydrate Research, 338*, 1235–1241.
Ciucanu, I., & Kerek, F. (1984). A simple and rapid method for the permethylation of carbohydrates. *Carbohydrate Research, 131*, 209–217.
Cunha, P. L. R., Vieira, Í. G. P., Arriaga, Ñ. M. C., de Paula, R. C. M., & Feitosa, J. P. A. (2009). Isolation and characterization of galactomannan from *Dimorphandra gardneriana* Tul. seeds as a potential guar gum substitute. *Food Hydrocolloids, 23*, 880–885.
Francis, F., Sabu, A., Nampoothiri, K. M., Ramachandran, S., Ghosh, S., Szakacs, G., et al. (2003). Use of response surface methodology for optimizing process parameters for the production of α-amylase by *Aspergillus oryzae*. *Biochemical Engineering Journal, 15*, 107–115.
Guo, B., Wang, Y., Sun, X., & Tang, K. (2008). Bioactive natural products from endophytes: A review. *Applied Biochemistry and Microbiology, 44*, 136–142.
Han, Y. W., & Clarke, M. A. (1990). Production and characterization of microbial levan. *Journal of Agricultural and Food Chemistry, 38*, 393–396.
Hineno, M. (1977). Infrared spectra and normal vibration of β-D-glucopyranose. *Carbohydrate Research, 56*, 219–227.
Jung, H. K., Hong, J. H., Park, S. C., Park, B. K., Nam, D. H., & Kim, S. D. (2007). Production and physicochemical characterization of β-glucan produced by *Paenibacillus polymyxa* JB115. *Biotechnology and Bioprocess Engineering, 12*, 713–719.
Kardošová, A., Ebringerová, A., Alföldi, J., Nosál'ová, G., Fraňová, S., & Hříbalová, V. (2003). A biologically active fructan from the roots of *Arctium lappa* L., var. *Herkules*. *International Journal of Biological Macromolecules, 33*, 135–140.
Lee, I. Y., Seo, W. T., Kim, G. J., Kim, M. K., Ahn, S. G., Kwon, G. S., et al. (1997). Optimization of fermentation conditions for production of exopolysaccharide by *Bacillus polymyxa*. *Bioprocess Engineering, 16*, 71–75.
Lim, J. M., Joo, J. H., Kim, H. O., Kim, H. M., Kim, S. W., Hwang, H. J., et al. (2005). Structural analysis and molecular characterization of exopolysaccharides produced by submerged mycelial culture of *Collybia maculata* TG-1. *Carbohydrate Polymers, 61*, 296–303.
Liu, J., Luo, J., Ye, H., Sun, Y., Lu, Z., & Zeng, X. (2009). Production, characterization and antioxidant activities in vitro of exopolysaccharides from endophytic bacterium *Paenibacillus polymyxa* EJS-3. *Carbohydrate Polymers*. doi:10.1016/j.carbpol.2009.03.046.
Lu, F., Sun, L., Lu, Z., Bie, X., Fang, Y., & Liu, S. (2007). Isolation and identification of an endophytic strain EJS-3 producing novel fibrinolytic enzymes. *Current Microbiology, 54*, 435–439.
Majumder, A., Singh, A., & Goyal, A. (2009). Application of response surface methodology for glucan production from *Leuconostoc dextranicum* and its structural characterization. *Carbohydrate Polymers, 75*, 150–156.
Madden, J. K., Dea, I. C. M., & Steer, D. C. (1986). Structural and rheological properties of the extracellular polysaccharides from *Bacillus polymyxa*. *Carbohydrate Polymers, 6*, 51–73.
Mattos, K. A., Jones, C., Heise, N., Previato, J. O., & Mendonça-Previato, L. (2001). Structure of an acidic exopolysaccharide produced by the diazotrophic endophytic bacterium *Burkholderia brasiliensis*. *European Journal of Biochemistry, 268*, 3174–3179.
Ogawa, K., Wanatabe, T., Tsurugi, J., & Ono, S. (1972). Conformational behaviour of a gel-forming (1 → 3)-β-D-glucan in alkaline solution. *Carbohydrate Research, 23*, 399–405.
Schwanninger, M., Rodrigues, J. C., Pereira, H., & Hinterstoisser, B. (2004). Effects of short-time vibratory ball milling on the shape of FT-IR spectra of wood and cellulose. *Vibrational Spectroscopy, 36*, 23–40.
Serrato, R. V., Sassaki, G. L., Cruz, L. M., Pedrosa, F. O., Gorin, P. A. J., & Iacomini, M. (2006). Culture conditions for the production of an acidic exopolysaccharide by the nitrogen-fixing bacterium *Burkholderia tropica*. *Canadian Journal of Microbiology, 52*, 489–493.
Serrato, R. V., Sassaki, G. L., Gorin, P. A. J., Cruz, L. M., Pedrosa, F. O., Choudhury, B., et al. (2008). Structural characterization of an acidic exoheteropolysaccharide produced by the nitrogen-fixing bacterium *Burkholderia tropica*. *Carbohydrate Polymers, 73*, 564–572.
Shih, I. L., Yu, J. Y., Hsieh, C., & Wu, J. Y. (2009). Production and characterization of curdlan by *Agrobacterium* sp. *Biochemical Engineering Journal, 43*, 33–40.
Shimamura, A., Tsuboi, K., Nagase, T., Ito, M., Tsumori, H., & Mukasa, H. (1987). Structural determination of D-fructans from *Streptococcus mutans*, serotype *b, c, e* and *f* strains, by ^{13}C-n.m.r. spectroscopy. *Carbohydrate Research, 165*, 150–154.
Staub, A. M. (1965). Removal of protein – Sevag method. *Methods in Carbohydrate Chemistry, 5*, 5–6.
Tadych, M., & White, J. F. (2009). Endophytic microbes. In M. Schaechter (Ed.), *Encyclopedia of microbiology* (pp. 431–442). New York: Academic Press.
Tajima, K., Uenishi, N., Fujiwara, M., Erata, T., Munekata, M., & Takai, M. (1998). The production of a new water-soluble polysaccharide by *Acetobacter xylinum* NCI 1005 and its structural analysis by NMR spectroscopy. *Carbohydrate Research, 305*, 117–122.
Tang, X. J., He, G. Q., Chen, Q. H., Zhang, X. Y., & Ali, M. A. M. (2004). Medium optimization for the production of thermal stable β-glucanase by *Bacillus subtilis* ZJF-1A5 using response surface methodology. *Bioresource Technology, 93*, 175–181.
Wack, M., & Blaschek, W. (2006). Determination of the structure and degree of polymerisation of fructans from *Echinacea purpurea* roots. *Carbohydrate Research, 341*, 1147–1153.
Wu, M., Wu, Y., Zhou, J., & Pan, Y. (2009). Structural characterisation of a water-soluble polysaccharide with high branches from the leaves of *Taxus chinensis* var. *mairei*. *Food Chemistry, 113*, 1020–1024.
Yoo, S. H., Yoon, E. J., Cha, J., & Lee, H. G. (2004). Antitumor activity of levan polysaccharides from selected microorganisms. *International Journal of Biological Macromolecules, 34*, 37–41.